Tunneling magnetoresistance and induced domain structure in Al_2O_3-based junctions

M. Hehn, O. Lenoble, D. Lacour, C. Féry, and M. Piécuch
Laboratoire de Physique des Matériaux, UMR CNRS 7556, Université H. Poincaré–Nancy 1, Boîte Postale 239, 54506 Vandoeuvre Les Nancy Cedex, France

C. Tiusan and K. Ounadjela
Institut de Physique et de Chimie des Matériaux de Strasbourg, 23 rue du Loess, F-67037 Strasbourg Cedex, France
(Received 1 July 1999; revised manuscript received 30 November 1999)

Magnetization reversal in sputtered Co and oxidized Co (CoOx) layers are studied using transport measurements and magneto-optic Kerr effect. When associated in a magnetic tunnel junction, the two magnetic layers show a strong ferromagnetic coupling. Using the tunnel magnetoresistive effect as a probe for micromagnetic studies, we show the existence of an unexpected domain structure in the soft Co layer. This domain structure originates from the duplication of the domain structure of the hard CoOx magnetic layer template into the soft Co layer via the ferromagnetic coupling.

I. INTRODUCTION

Since the discovery of a tunnel magnetoresistance (TMR) effect at room temperature in oxide barrier based magnetic tunnel junctions, this research area is the subject of intense developments with many possible application prospects. The numerous studies devoted to different aspects of this topic permit to get a better understanding of the fundamentals of spin polarized tunneling transport. Up to now, much attention has been paid on the study of the tunnel barrier properties and their optimization during the fabrication procedure. Indeed, this part of the junction is subjected to many diseases and some of them have been already addressed: natural[1] or artificial[2] defects, roughness of the barrier,[3,4] depth chemical homogeneity[5] and under or over oxidation of the barrier.[6] In contrast, since the forerunner model proposed by Jullière[7] which predicts the dependence of the TMR signal with the magnetic electrode polarization and its experimental proof, less attention has been concentrated on topics related to the use of magnetic electrodes. However, many other effects such as magnetization reversal processes, domain formation and implication of the domain structure in each magnetic layer in contact with the tunnel barrier on the TMR signal height have not been considered so far or have only recently emerged.[8–10] For instance, it has been shown that the existence of a domain structure in hard magnetic layers may induce extra current channels in TMR junctions due to the current perpendicular to plane (CPP) geometry.[10] The amount of shortened tunnel current, directly dependent on the domain structure, may rule out any potential applications as memory or heads applications.

In this paper, we report the relationship between tunnel transport and magnetic domain structure which occurs during the reversal of the magnetic layers in Co(10 nm)/AlOx/CoOx(10 nm) tunnel junctions. Tunnel junctions appear to be good candidates to study the magnetization reversal or the domain structure of ferromagnetic layers (FL's) in contact with the barrier because of the large sensitivity of the spin dependent tunnel current to nanoscale magnetic fluctuations. When the reversal of either the soft layer or the hard layer is known, it allows to extract the magnetic behavior of the other magnetic layer. From the measurements of the TMR curves in Co(10 nm)/AlOx/CoOx(10 nm) tunnel junctions, an unexpected domain structure in the soft cobalt (Co) layer has been evidenced. This domain structure is induced from the hard oxidized Co (CoOx) magnetic layer template via a strong indirect ferromagnetic coupling.

II. EXPERIMENTAL PROCEDURES

Single films and junctions are deposited onto float-glass substrates maintained at room temperature in an *Alcatel SCM 650* automated sputtering apparatus. 99.95% pure Co and aluminum (Al) targets are mounted on respectively 10 cm diameter rf and dc magnetron cathodes. The substrate-to-target distance is set to 10 cm. The base pressure is less than 5×10^{-7} mbar and 99.999% purified argon is introduced into the chamber through a pressure-regulated valve up to an operating pressure fixed to 5×10^{-3} mbar. All films are deposited in the dynamic mode: the substrate is scanned over the cathodes at 2 rpm in the case of Co and 4 rpm in the case of Al. The power applied by the generator to the target is chosen to have 3.0 Å/scan deposition rate for both Co and Al. To obtain the oxidized Al (AlOx) barrier and CoOx electrode, the oxidation is realized just after deposition of the metallic Al or Co layer using a dc glow discharge under a pure 10^{-1} mbar O_2 plasma in the sputtering load-lock. The samples are transferred to this chamber without breaking the vacuum.

To prepare junctions suitable for current perpendicular to plane (CPP) transport geometry measurements, we have used contact masks made in a 100 μm thick CuBe foil which allow us to prepare 16 junctions at each run on a sample. The patterning of the CuBe foil is achieved by a standard chemical etching technique with a path width of 200 μm. In the first place, Cr/Au contacts are evaporated onto each 20 $\times$20 mm^2 float-glass substrate. Then, the masks are sequentially set close to the substrate. Samples are transferred back to the load-lock for each *ex situ* contact mask change. Then, the load-lock is quickly vented with nitrogen, the mask is

changed and the load-lock is pumped down so that, the air exposure is less than 2 min. Details on the junction geometry can be found elsewhere.[11] Electrical resistivity and magnetoresistance are measured with a standard two-probe dc technique. Magnetization curves of the single magnetic films and the junctions are recorded at room temperature with a magneto-optic Kerr effect (MOKE) apparatus operating with a 6328 Å He-Ne laser in the longitudinal geometry.

III. MAGNETIZATION CURVES AND REVERSAL IN THE SOFT AND HARD MAGNETIC ELECTRODES

Tunnel magnetoresistance relates to the fact that the tunneling probability of electrons in a hybrid ferromagnetic/insulator/ferromagnetic layered structure depends on the relative orientation of the two FL magnetizations. This implies a pair of FL's for which the orientation of each magnetization can be reversed independently. For this purpose, we take advantage of the experimental setup used to grow our samples. Initially used to get films with uniform thickness, substrates are scanned over the cathodes in a dynamic mode in order to induce a small morphological uniaxial anisotropy (H_A). This first step leads to FL with square Kerr magnetization curves ($\theta-H$ curves) when measured along the easy axis with a coercive field (H_c) around 30 Oe. In a second step, the hard layer (the topmost in the three layers structure), grown in the same conditions, is 1 min oxidized using the experimental conditions and setup optimized to make up the tunnel barriers. After this oxidation, H_c increases drastically to values around 110 Oe at room temperature and the $\theta-H$ curves keep a squarelike shape, rounded for applied fields around H_c. The oxidation has then two effects on the magnetization reversal; (i) the switching of the magnetic layer is less abrupt and occurs in a field range of several tens of oersteds while the magnetization remanence (M_r/M_s) maintains a high value (about 95%), and (ii) the coercive field is increased by a factor of 4. These changes could not be explained by simple arguments.[12]

The origin of the Co layer hardening after oxidation and the change in the magnetization reversal mechanism have been addressed using magnetic force microscopy with an *in situ* applied field and anisotropy magnetoresistance (AMR) measurements.

In this last case, measurements have been performed on the junction electrodes individually probed using the typical cross architecture of the junction. Since both electrodes have parallel easy axis and the junction has a cross geometry, the Co (respectively CoOx) electrode has its easy magnetization axis perpendicular (respectively parallel) to its length. As far as the pure Co layer is concerned (bottom electrode), no evidence of a magnetization component perpendicular to H_A is observed during the reversal when the field is applied along the easy axis [Fig. 1(a), $-\bigcirc-$]. Considering the low value of H_c and the squareness of the $\theta-H$ curve, the magnetization reverses its direction by nucleation and propagation of domain walls.

The reversal of the top electrode appears to be substantially different after oxidation of the Co layer. The AMR response shown in Fig. 1(b) with the magnetic field parallel ($-\bigcirc-$) and perpendicular ($-\bullet-$) to H_A is consistent with a reversal occurring through the appearance of ripples domain structures.[13] When the value of the field applied along the easy axis is reduced from positive saturation to zero, magnetization rotates continuously in the film plane in a reversible process and a component perpendicular to H_A appears. The magnetic moments are then aligned within an angle bisected by the direction of the positive saturation field. On a microscopic scale, the sense of rotation is defined by the angle between the local effective magnetocrystalline anisotropy and the external applied field imposing that regions distributed over the whole sample may rotate clockwise or counterclockwise. When the applied field is reversed in the negative direction, regions with the lowest local effective anisotropy switch first their magnetization in a direction close to the one of the negative applied field. This reversal leads undoubtedly to reversals of other regions coupled either by exchange or by dipolar interactions. This generates regions with main magnetization oriented in the negative direction which coexist with regions with main magnetization oriented in the positive field direction. Increasing the negative applied field increases the proportion of reversed magnetized regions until negative saturation is reached.

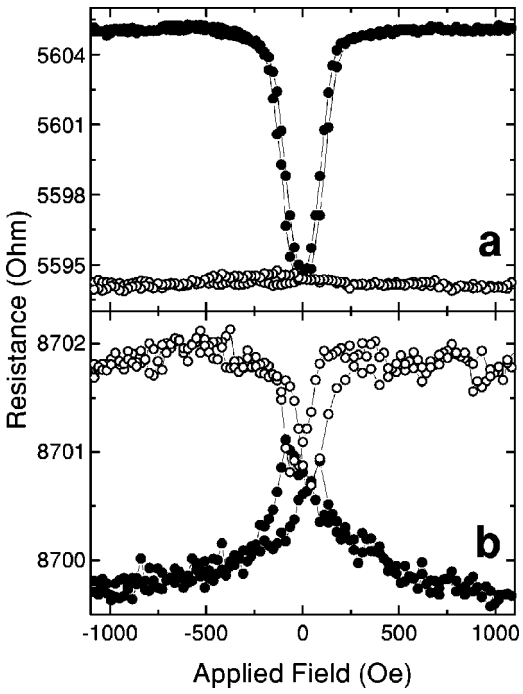

FIG. 1. Anisotropy of magnetoresistance measurements performed on the Co (a) and CoOx (b) junction electrodes. The Co (respectively CoOx) electrode has its easy axis of magnetization perpendicular (respectively parallel) to its length. Measurements are made with the field applied parallel ($-\bigcirc-$) and perpendicular ($-\bullet-$) to the easy axis of magnetization.

This reversal mechanism was supported using magnetic force microscopy with an *in situ* applied field.[10,14] In the field range of interest (from 0 to -300 Oe after positive saturation), no correlated walls could be observed during the magnetization reversal, only small dipolar contrasts compatible with small leakage fields. The MFM pattern is mainly composed of lines without contrast directed in the applied field direction and a white and black checkerboard, the position of each contrast depending on the applied field. These last contrasts are due to the lateral fluctuation of the magnetization

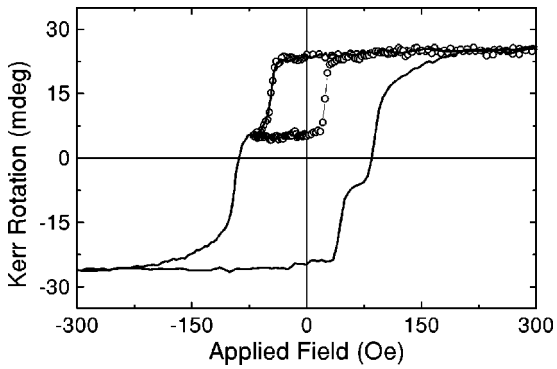

FIG. 2. Complete $(-)$ and minor $(-\bigcirc-)$ magnetization loops measured by longitudinal Kerr effect directly on a Co(10 nm)/Al(1.5 nm, ox 1 mn, 45 s)/Co(10 nm, ox 1 mn) tunnel junction with 200 μm lateral size. The shift of the minor loop towards the negative applied fields exemplifies the ferromagnetic coupling between the magnetic electrodes.

component perpendicular to H_A and their analysis will be published elsewhere.[15] The modification of the reversal mechanism must be directly related to the oxidation process. Indeed, the diffusion of oxygen in the grain boundaries during the oxidation process weakens the exchange coupling between grains and therefore reduces the averaging of the randomly directed anisotropy fields of various grains. This fact has been shown by Berkov *et al.*[16] to be at the origin of the appearance of a ripple domain structure which leads to the increase of H_c and the decrease of M_r/M_s.

IV. MAGNETIZATION CURVE AND REVERSAL IN THE SOFT AND HARD MAGNETIC ELECTRODES SEPARATED BY A THIN TUNNEL BARRIER—TMR IN THESE JUNCTIONS

The next section of the paper is devoted to the analysis of the magnetization reversal of the two FL's when they are used as electrodes in a magnetic tunnel junction. Therefore, a complete $\theta-H$ curve measured along H_A directly on a 200 μm lateral size junction is presented in Fig. 2. It appears clearly that the coercive field of the Co layer is increased up to 45 Oe while the H_c of the CoOx layer is decreased down to 90 Oe. In fact, the intrinsic H_c of each FL has not changed but the reversals of the FL's are mutually influenced due to their proximity. This is exemplified by the minor loop shown in Fig. 2. As can be seen on the branch which extends from -75 O*e* to positive saturation, the reversal of the soft Co layer occurs for an applied field of $+25$ O*e*. The loop corresponding to the reversal of the soft Co layer is shifted by a bias field of -10 O*e* corresponding to a ferromagnetic coupling with the hard CoOx layer. This coupling can be attributed to the orange-peel effect originating in a coherent corrugation of the top and bottom interfaces of the barrier.[17] As it will be shown in the following, this ferromagnetic coupling has a strong influence on the magnetization reversal of the soft Co detection layer when the hard CoOx layer includes a domain structure.

The magnetotransport properties of Co(10 nm)/Al(t_{Al} nm, t_{ox} mn)/Co(10 nm, ox 1 mn) have been studied as a function of t_{Al}, the deposited Al thickness, and t_{ox}, the oxidation time. Since the TMR signal is known to be strongly dependent on the under and overoxidation of the Al layer, an optimum t_{Al} is expected for a given t_{ox}. For our oxidation technique and t_{ox} equal to 1 mn 30 s, the optimum Al thickness is 15 Å for which the TMR signal[18] at room temperature is equal to 9% and the mean junction resistance to 120 kΩ. On the one hand, when t_{Al} is increased to 18 Å, the resistance shows a slight increase (of about 15%) while the TMR signal decreases to 7%. On the other hand, when t_{Al} is decreased to 12 Å, the TMR signal and the resistance drop to about 5% and 40 kΩ, respectively. The TMR signal shows the well known decrease with the applied voltage with a characteristic $|V_{1/2}|$, the applied voltage for which the TMR signal is reduced by a factor of two, of 0.2 to 0.4 V depending on the polarity of the junction. Brinkman's theory of tunneling[19] was applied to estimate the effective barrier height, Φ, and thickness, t_{eff}. No clear correlation could be observed between Φ, with values above 0.8 eV and less than 1.2 eV, and t_{ox} but the fitted t_{eff} are always in good agreement with t_{Al}. Junctions with the best magnetotransport properties have been measured at low temperature, down to 4.2 K. Their resistance increases linearly as temperature T is decreased and saturates for T less than 75 K at a value two times larger than at room temperature. In a same manner, the TMR signal shows an increase of 30% and reached 12% for $t_{\mathrm{Al}}=15$ Å.

V. EFFECT OF THE FERROMAGNETIC COUPLING BETWEEN THE ELECTRODES ON THE TMR SIGNAL

The following aims to show how the ferromagnetic coupling between two electrodes strongly influences the magnetization reversal of the soft Co layer when the hard CoOx layer includes a domain structure. Since tunneling current decreases exponentially with the distance through the barrier, the preferential conduction channels are the shortest paths for electrons to travel across the insulator. Therefore, the most important factor which determines the magnitude of the spin polarized tunneling current is the relative local orientation of the ferromagnetic moments directly across the barrier. We use this large sensitivity to local magnetization fluctuations of the spin dependent tunnel current and the knowledge of the reversal of the hard magnetic layer to infer the induced domain structure in the soft pure Co layer.

Complete $(-)$ and minor $(-\bigcirc-)$ characteristic TMR loops are shown in Fig. 3 measured on a Co(10 nm)/Al(1.8 nm, ox 1 mn)/Co(10 nm, ox 1 mn) tunnel junction with 200 μm lateral size. The features appearing in the minor loop are reproducible [measured on several Co(10 nm)/Al(1.8 nm, ox 1 mn)/Co(10 nm, ox 1 mn) junctions] but dependent on t_{Al} and t_{ox}.[15] After saturation at 500 Oe, the applied field is decreased down to -500 Oe (complete cycle) or to H_{rev} (minor cycle). The resistance jumps, $\Delta R(H_c(\mathrm{Co}))$, occurring at the effective H_c of the soft Co layer, $H_c(\mathrm{Co})$, are equal in both cases. By reversing the applied field and increasing its value from -500 Oe or from H_{rev} towards 500 Oe, the two cycles appear to be completely different. In the case of the complete negative saturation (major cycle), the cycle is symmetric and therefore holds two resistance jumps. As far as the minor loop is concerned, three resistance jumps with different signs appear at some fields named H_1,H_2 and H_3, which are different than $H_c(\mathrm{Co})$,

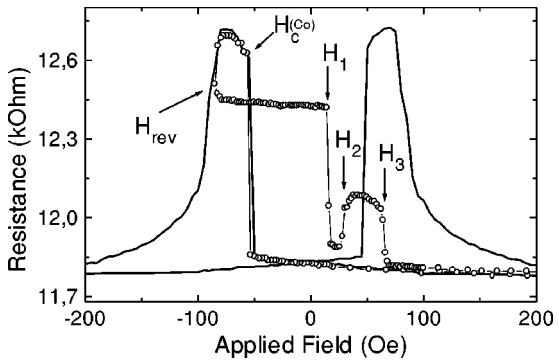

FIG. 3. Complete $(-)$ and minor $(-\bigcirc-)$ tunnel magnetoresistance loops measured on a Co(10 nm)/Al(1.8 nm, ox 1 mn)/Co (10 nm, ox 1 mn) tunnel junction with 200 μm lateral size. By reversing the negative applied field at some H_{rev} on the minor loop, three jumps with different signs appear at some fields H_1, H_2, and H_3.

H_c^{int}(Co)—the intrinsic H_c of the Co layer—or than the effective H_c of the hard CoOx layer, H_c(CoOx).

In order to shed light on the phenomena responsible for the additional jump, the magnitudes of the different resistance jumps have been studied as a function of H_{rev}, the value at which the applied field, H, is reversed. The variation of the resistance jump amplitudes for the previous defined applied fields H_c(Co) $(-\bullet-)$, $H_1(-\square-)$, and H_2 (filled black square) are reported in Fig. 4. The last curve $(-\bigcirc-)$ added to the plot is the sum of the absolute values of the resistance jumps at H_1, $\Delta R(H_1)$, and at H_2, $\Delta R(H_2)$. Several trends can be extracted from this figure. When $|H_{\text{rev}}|$ is between 45 and 85 Oe [between H_c(Co) and H_c(CoOx)], only one resistance jump is observed with value equal or slightly less than $\Delta R(H_c(\text{Co}))$. This jump is easily attributed to the own reversal of the soft Co layer. As H_{rev} decreases towards negative fields, $\Delta R(H_1)$ decreases while $\Delta R(H_2)$ increases. Their variations appear to be correlated since their sum remains constant, 15% lower than $\Delta R(H_c(\text{Co}))$. When $|H_{\text{rev}}|$ exceeds 165 Oe, $\Delta R(H_1)$ is reduced to zero and remains constant while $\Delta R(H_2)$, H_2, and H_3 continuously converge towards $\Delta R(H_c(\text{Co}))$, H_c(Co), and H_c(CoOx), respectively.

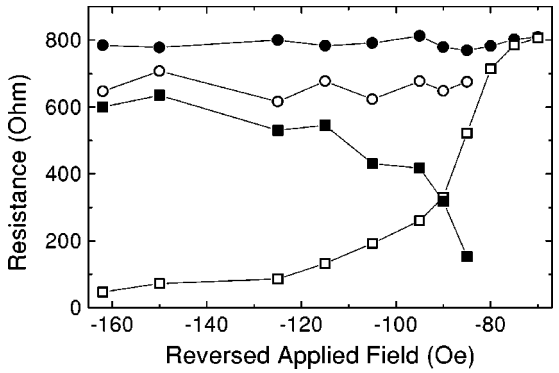

FIG. 4. Variation of the amplitude of the resistance jumps measured for an applied field H_c (Co)(●), H_1(□), and H_2 (filled black square) as a function of the reversing negative applied field H_{rev}. The last curve (○) is a plot of the sum of the absolute value of the resistance jumps at H_1 and H_2.

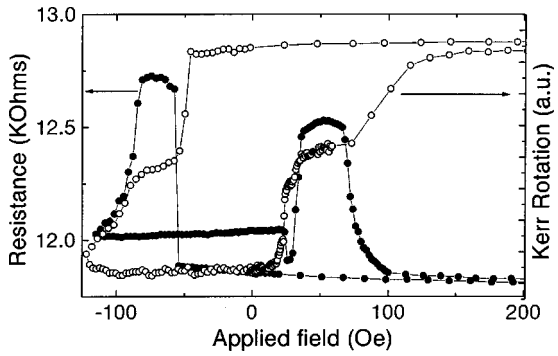

FIG. 5. Comparison between a minor tunnel magnetoresistance loop $(-\bullet-)$ and a minor magnetization loop measured by longitudinal Kerr effect directly on a Co(10 nm)/Al(1.8 nm, ox 1 mn 30 s)/Co(10 nm, ox 1 mn) tunnel junction with 200 μm lateral size $(-\bigcirc-)$. The reduction of resistance for applied fields between 22 and 34 Oe is correlated to the appearance of a plateau in the minor magnetization loop. This plateau disappears on the complete magnetization loop as exemplified in Fig. 2.

Particularly interesting is the fact that for applied fields between H_1 and H_2, the resistance of the junction is close to the one measured when the magnetizations of the two magnetic electrodes are in a parallel configuration. Therefore, directly across the barrier, the magnetization of the two magnetic electrodes are locally parallel even if the hard magnetic layer is far from magnetic saturation. As a consequence, the domain structure of the hard CoOx layer is duplicated in the soft pure Co layer. An evidence of the perturbation of the soft Co electrode reversal is given in Fig. 5 where a minor tunnel magnetoresistance loop $(-\bullet-)$ and a minor magnetization loop measured on a tunnel junction $(-\bigcirc-)$ are compared. The reduction of resistance for applied fields between 22 and 34 Oe is correlated to the appearance of a plateau in the magnetization reversal of the soft Co layer in the minor magnetization loop. This plateau corresponds to a field window for which the duplicated domain structure is stable in the soft Co layer while it disappears on the complete magnetization loop as exemplified in Fig. 2. The existence of such domain structure in the soft layer creates low resistance paths which partially shorten the tunnel current and hence reduces the overall TMR ratio.

A model of domain structure is sketched in Fig. 6 to explain the main features of the minor TMR curves observed experimentally. It relays on the knowledge of the reversal of the hard magnetic CoOx layer and the strength of the ferromagnetic coupling between the two electrodes. As described in a previous section, when H, directed along H_A in the direction opposite to the positive saturating field, has values around $-H_c$(CoOx) (in the case of the present MTJ between -85 Oe and -160 Oe) a domain structure exists in the CoOx electrode while the soft Co layer is saturated in the negative field direction. This domain structure consists of regions with main magnetization oriented in the negative field direction created when $|H|$ exceeds 85 Oe which coexist with regions with main magnetization oriented in the positive field direction [Fig. 6(a)]. As mentioned above, increasing the negative applied field increases the density of reversed magnetized regions until negative domain saturation is reached at $|H|$ around 160 Oe.

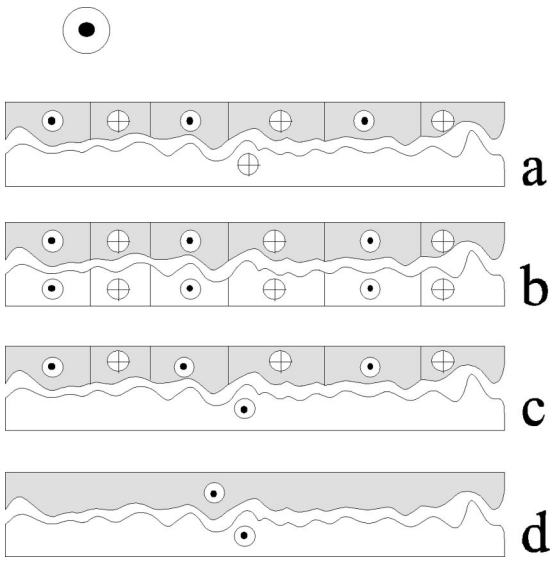

FIG. 6. Sketch showing the evolution of the domain structure in each magnetic layer, the soft Co layer (bottom layer, white) and the hard CoOx layer (top layer, gray scale). The symbols $\odot$ and $\otimes$ represent the main magnetization in each domain (oriented perpendicular to the paper sheet) respectively opposite and along the positive saturating field (represented by the big $\odot$ outside the sketch). After a positive saturation, the applied field is decreased and reversed until H_{rev} is reached. At this field, the soft Co layer is saturated and a domain structure remains in the hard CoOx layer (a). Reversing the field in the positive direction, the reversal of the soft Co layer occurs in two steps. First, the magnetization of regions located under domains in the hard CoOx layer with magnetization oriented in the positive saturating field direction reverses at a field H_1 (b). Then, at H_2, the Co layer reaches its positive saturation state (c). Finally, the CoOx layer saturates at H_3 for which the resistance is minimal (d).

As H is reversed from H_{rev} towards the positive fields, regions of the soft layer which are located over domains in the CoOx layer with main magnetization oriented in the positive field direction experience a local field equal to $H+H_f$, where H_f represents the ferromagnetic field coupling between the two electrodes. Therefore, these regions will rotate first for an applied field of approximately $H_c^{\mathrm{int}}(\mathrm{Co})-H_f$. In fact, the reversal field is slightly higher due to the energy needed to include domain walls in the soft Co layer. After reversal and as exemplified in Fig. 6(b), the two magnetic electrodes hold the same domain structure. A part from the magnetization inside the walls, locally in both layers, magnetizations are parallel. Therefore, the junction resistance decreases with a jump of $\Delta R(H_1)$ and is nearly minimal. This correlated domain structure can be observed in these samples because the energy spend to create domain walls is less than the gain in energy linked to regions ferromagnetically aligned. A further increase of H leads to the reversal of regions of the soft layer which are located over domains in the CoOx layer with main magnetization oriented in the negative field direction and experience a local field equal to $H-H_f$. Indeed, these regions will switch for an applied field of approximately $H_c^{\mathrm{int}}(\mathrm{Co})+H_f$. In fact, the reversal field is slightly smaller due to the gain in energy arising from the disappearance of walls in the Co layer. After reversal and as exemplified in Fig. 6(c), the soft layer is in a single domain state while the domain structure remains in the hard layer. Locally in both layers, magnetizations are either parallel or antiparallel and this last magnetic configuration contributes to the increase of the junction resistance $\Delta R(H_2)$. A further increase of H leads finally to the saturation of the CoOx magnetization [Fig. 6(d)]. Here again, locally in both layers, magnetizations are parallel and walls have disappeared. Therefore, resistance decreases and reaches its value at saturation. The magnitude of this last resistance jump $\Delta R(H_3)$ is close to the difference $R(H_c(\mathrm{Co}))-R(H_{\mathrm{rev}})$, where $R(H_c(\mathrm{Co}))$ and $R(H_{\mathrm{rev}})$ are the resistances measured at $H_c(\mathrm{Co})$ and H_{rev}, respectively, indicating that the domain structure present in the CoOx layer remains approximately constant when the applied magnetic field increases from H_{rev} up to H_3.

In the light of this model, the behavior of $\Delta R(H_i)$ ($i=1$, 2 and 3) as a function of H_{rev} can be explained. As mentioned above, when H_{rev} is between -85 and -160 Oe and when its value decreases, the density of reversed magnetized regions increases in the CoOx electrode. Therefore, $R(H_{\mathrm{rev}})$ decreases and consequently $\Delta R(H_1)$ also decreases. The gain in resistance at H_2 is directly proportional to the density of domains in the CoOx layer with negative main magnetization. By increasing $|H_{\mathrm{rev}}|$, their density increases and consequently $\Delta R(H_2)$ decreases too. Finally, increasing $|H_{\mathrm{rev}}|$ up to 160 Oe, H_1 and H_2 get close to $H_c(\mathrm{Co})$ and H_3 gets close to $H_c(\mathrm{CoOx})$.

VI. CONCLUSIONS

In this paper, we present results on the magnetic properties of Co and CoOx electrodes and on the magnetotransport properties of Co(10 nm)/AlOx/CoOx(10 nm) tunnel junctions. We have demonstrated that the oxidation of the Co electrode leads to a drastic change of its reversal mechanism and to the appearance of a ripple domain structure which induces an increase of the coercive field. When a junction is constituted with these two electrodes separated by an AlOx layer, a dipolar interaction takes place leading to a decrease of the difference between both coercive fields. The main purpose of this paper is to report, for the first time, on induced domain structure in the soft magnetic layer duplicated from the hard magnetic layer template by a ferromagnetic type coupling. Then, we characterized magnetotransport properties of these junctions in order to study the magnetization reversal of the soft Co electrode. In fact, spin dependent tunneling current is severely affected by local magnetization fluctuations and the knowledge of the magnetic structure in one electrode (the hard electrode) must conduct to the understanding on the magnetization reversal of the second electrode (the soft electrode).

ACKNOWLEDGMENTS

The authors thank J.-F. Bobo, M. Demand, J. Latriche, L. Moreau, J.-G. Mussot, and C. Senet for their technical support, and C. Bellouard, G. Marchal, A. Schuhl, and R. L. Stamps for many fruitful discussions and for help with the experiments.

[1] C.H. Shang, J. Nowak, R. Jansen, and J.S. Moodera, Phys. Rev. B **58**, R2917 (1998).
[2] R. Jansen and J.S. Moodera, J. Appl. Phys. **83**, 6682 (1998).
[3] F. Bardou, Europhys. Lett. **39**, 239 (1997).
[4] V. Da Costa, F. Bardou, C. Bal, Y. Henry, J.-P. Bucher, and K. Ounadjela, J. Appl. Phys. **83**, 6703 (1998).
[5] R.C. Sousa, J.J. Sun, V. Soares, P.P. Freitas, A. Kling, M.F. da Silva, and J.C. Soares, Appl. Phys. Lett. **73**, 3288 (1998).
[6] J.S. Moodera, E.F. Gallagher, K. Robinson, and J. Nowak, Appl. Phys. Lett. **70**, 3050 (1997).
[7] M. Jullière, Phys. Lett. **54A**, 225 (1975).
[8] C.L. Platt, B. Dieny, and A.E. Berkowitz, J. Appl. Phys. **81**, 5523 (1997).
[9] R.E. Dunin-Borkowski, M.R. McCartney, D.J. Smith, S. Gider, B.U. Runge, and S.S. Parkin, J. Appl. Phys. **85**, 4815 (1999).
[10] C. Tiusan, T. Dimopoulos, M. Hehn, V. Da Costa, Y. Henry, H. A. M. van den Berg, and K. Ounadjela, Phys. Rev. B **61**, 580 (2000).
[11] Ch. Féry, L. Hennet, O. Lenoble, M. Piecuch, E. Snoeck, and J.F. Bobo, J. Phys.: Condens. Matter **10**, 6629 (1998).
[12] This increase in H_c cannot be explained only by the reduction of the magnetic effective layer thickness. Indeed, even if an increase of 50% in H_c is observed as the thickness of a nonoxidized Co layer is decreased from 10 to 5 nm, another mechanism must be invoked. Therefore, we have studied the magnetic susceptibility of the CoOx layer as a function of temperature. The Néel and blocking temperatures of this thin layer appear to be below 80 K. So, at room temperature, an eventual antiferromagnetic CoOx layer cannot be called to explain the H_c increase.
[13] K.D. Leaver, Thin Solid Films **2**, 149 (1968).
[14] C. Tiusan and M. Hehn (private communication).
[15] M. Hehn, O. Lenoble, D. Lacour, A. Schuhl, C. Tiusan and K. Ounadjela (unpublished).
[16] D.V. Berkov and N.L. Gorn, Phys. Rev. B **57**, 14 332 (1998).
[17] L. Néel, C. R. Acad. Sci. URSS **255**, 1676 (1962).
[18] In this article, the TMR signal is defined as the ratio of the difference of resistance in the parallel and antiparallel magnetization configurations and the resistance in the antiparallel magnetization configuration.
[19] W.F. Brinkman, R.C. Dynes, and J.M. Rowell, J. Appl. Phys. **41**, 1915 (1971).